



## ORIGINAL ARTICLE

# Ion release and local effects of titanium metal particles from dental implants: An experimental study in rats

Jorge Toledano-Serrabona<sup>1,2</sup> | Octavi Camps-Font<sup>1,2</sup> | Diogo Pompéu de Moraes<sup>3,4,5</sup> | Mario Corte-Rodríguez<sup>3,4</sup> | María Montes-Bayón<sup>3,4</sup> | Eduard Valmaseda-Castellón<sup>1,2</sup> | Cosme Gay-Escoda<sup>1,2</sup> | M. Ángeles Sánchez-Garcés<sup>1,2</sup>

<sup>1</sup>Department of Oral Surgery and Implantology, Faculty of Medicine and Health Sciences, University of Barcelona, Barcelona, Spain

<sup>2</sup>Bellvitge Biomedical Research Institute (IDIBELL), Barcelona, Spain

<sup>3</sup>Department of Physical and Analytical Chemistry, Faculty of Chemistry, University of Oviedo, Oviedo, Spain

<sup>4</sup>Instituto de Investigación Sanitaria del Principado de Asturias (ISPA), Oviedo, Spain

<sup>5</sup>Institute of Chemistry, Universidade Federal do Rio Grande do Sul, Porto Alegre, Rio Grande do Sul, Brazil

## Correspondence

Jorge Toledano-Serrabona, School of Medicine and Health Sciences, Campus de Bellvitge, University of Barcelona, C/ Feixa Llarga s/n; Pavelló Govern, 2<sup>a</sup> planta, Despatx 2.9, 08907 – L'Hospitalet de Llobregat (Barcelona), Spain.  
Email: [jorgetoledano25@gmail.com](mailto:jorgetoledano25@gmail.com)

## Abstract

**Background:** The objective of this study was to evaluate the accumulation of ions in blood and organs caused by titanium (Ti) metal particles in a mandibular defect in rats, together with a description of the local reaction of oral tissues to this Ti alloy debris.

**Methods:** Twenty Sprague-Dawley rats were randomly distributed into three groups: an experimental group with a mandibular bone defect filled with metallic debris obtained by implantoplasty; a positive control group; and a negative control group. Thirty days after surgery, the rats were euthanized and perilesional tissue surrounding the mandibular defect was removed, together with the lungs, spleen, liver, and brain. Two blood samples were collected: immediately before surgery and before euthanasia. The perilesional tissue was histologically analyzed using hematoxylin-eosin staining, and Ti, aluminum, and vanadium ion concentrations in blood and organs were measured by TQ-ICP-MS. Descriptive and bivariate analyses of the data were performed.

**Results:** All rats with implanted metal debris showed metal particles and a bone fracture callus on the osseous defect. The metal particles were surrounded by a foreign body reaction characterized by the presence of histiocytes and multinucleated giant cells (MNGCs). The experimental group had a significant higher concentration of Ti ions in all studied organs except lung tissue ( $p < 0.05$ ). In addition, there were more V ions in the brain in the experimental group ( $p = 0.008$ ).

**Conclusions:** Although further studies are required to confirm the clinical relevance of these results, Ti metal particles in the jaw might increase the concentration of metal ions in vital organs and induce a foreign body reaction.

## KEYWORDS

implantoplasty, ion release, metal particles, peri-implantitis, Ti6Al4V, titanium



## 1 | INTRODUCTION

Commercially pure titanium (Ti) or Ti alloys are the most commonly used metallic materials in dental implants.<sup>1</sup> Despite implants have proven to be a successful treatment to restore function and esthetics in edentulous patients,<sup>2</sup> the increasing number of peri-implant diseases has become a growing concern in implant dentistry.<sup>3</sup>

Although it is well documented that peri-implantitis is an inflammatory condition caused by bacterial plaque,<sup>4</sup> there are other factors such as Ti metal particles that have been suggested as a contributor factor.<sup>5,6</sup> Ti-based implants are biocompatible due to formation of a protective Ti oxide layer. This stable passive film protects the surface of the dental implant from corrosion.<sup>7,8</sup> However, an acid environment or implant polishing can reduce the corrosion resistance of the material until the loss of the Ti oxide layer.<sup>8,9</sup> This fact facilitates the release of nanodebris and soluble metal ions that might induce adverse tissue reactions.<sup>10</sup>

The presence of nanoparticulated metal debris in the peri-implant tissues has been previously described.<sup>11</sup> In addition, the presence of molecules, such as citrate or tartrate in biological fluids might also generate “soluble” forms of Ti (Ti-citrate or Ti-tartrate).<sup>12</sup> Therefore, ions and particles are two different forms of Ti that coexist in the peri-implant environment. Likewise, the effects of the release of these metal ions and nanoparticles into the medium are still unknown.<sup>5,13,14</sup> On the other hand, the interaction between Ti metal particles and peri-implant tissues still raises controversy.<sup>15</sup> Albrektsson et al.<sup>16</sup> suggested that this metal debris triggers a foreign body reaction, while others<sup>17,18</sup> reported that Ti particles induce a pro-inflammatory response.

The primary objective of this experimental animal study was to determine whether accumulation of Ti metal particles from dental implants in mandibular bone defects of rats results in a significant translocation and accumulation of Ti, aluminum (Al) and vanadium (V) ions in blood, liver, spleen and brain. The secondary objective was to analyze the response of perilesional bone and mucosal tissue to the presence of such Ti metal particles.

## 2 | MATERIALS AND METHODS

### 2.1 | Animal model

The present study followed the ARRIVE guidelines for conducting animal studies,<sup>19</sup> and was approved by the Ethics Committee for Animal Experimentation of the University of Barcelona (CEEA-UB) (Spain), under identification number 10799.

A randomized experimental study was carried out in 20 Sprague-Dawley rats. Adult male and female (proportion 1:1) ex-reproductive rats aged 6–8 months and with a weight of 380–450 g were included in the study. All animals were housed under standard conditions of 12-h light-dark cycles at a temperature of  $22 \pm 2^\circ\text{C}$  and a relative humidity of  $50\% \pm 10\%$ .

### 2.2 | Sample size calculation

In order to compare the intervention with a reference,<sup>20</sup> the sample size was calculated using a bilateral *t*-test for independent groups with a power of 90% and an alpha error of 5%, using an effect size of 1.05 and a common standard deviation (SD) of 0.62. Two experimental rats were added to the experimental group to compensate possible losses. Then, the rats were randomized to one of three groups: an experimental group (10 rats with a unilateral mandibular defect filled with metal debris); a positive control group (eight rats with an empty unilateral mandibular defect); and a negative control group (two rats with no mandibular defect).

### 2.3 | Randomization and concealment

A table of random numbers was generated using Stata14 (StataCorp, College Station, TX, USA) for random allocation. To ensure concealment of allocation from the surgeon, an independent investigator (O.C-F.) allocated the rats using sealed, opaque and numbered envelopes. Since the negative control rats did not undergo surgery, their envelopes were labeled on the outside. The envelopes were opened sequentially just after the mandibular bone defects were made.

### 2.4 | Preparation of metal debris

Metal particles obtained from implantoplasty of Ti-6Al-4V dental implants (Avinent Implant System S.L., Santpedor, Spain) were collected. The authors followed a standardized implantoplasty protocol used in humans and previously described by Costa-Berenguer et al.<sup>21</sup> In order to standardize the procedure, all implantoplasty procedures were performed by a single investigator (J.T.-S.). Implantoplasty was carried out to remove the threads of  $4.8 \times 13$  mm dental implants (Coral E.C., Avinent Implant System S.L., Santpedor, Spain). The implant surface was sequentially modified with a fine-grained tungsten carbide bur (H379.314. 014, KOMET GmbH & Co. KG, Lemgo, Germany) and two silicon carbide polishers (9608.314.030 and 9618.314.030, KOMET GmbH & Co. KG, Lemgo, Germany).

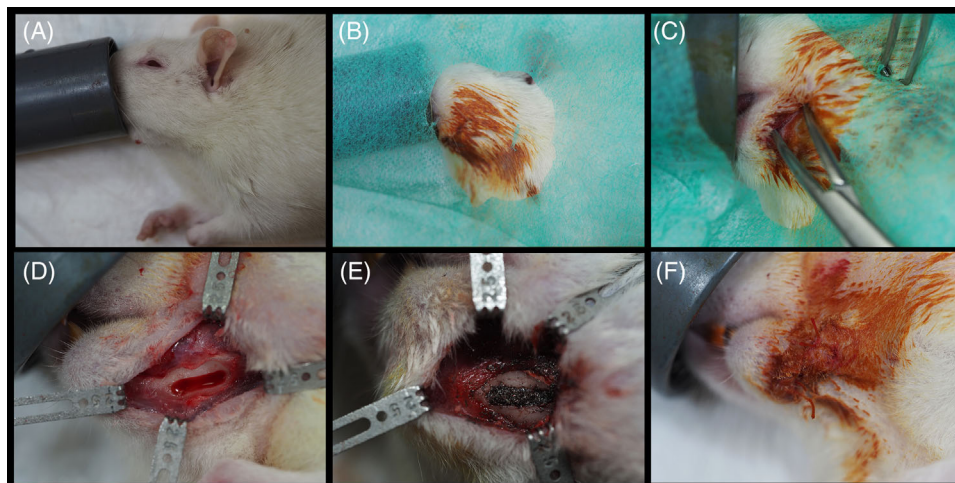


**FIGURE 1** Surgical procedure. Inhalation anesthesia (A), disinfection of the surgical area (B), incision and dissection (C), bone defect (D), metal particles filling bone defect (E), and suture (F)

## 2.5 | Surgical protocol

The surgical procedure was performed by a single experienced investigator (M.A.S.-G.). Anesthesia was induced in a chamber using 5% isoflurane (Forane, Abbott Laboratories, Madrid, Spain) and a continuous oxygen flow of 5 L/min. Buprenorphine (Buprex, RB Pharmaceuticals Ltd., Slough, Berkshire, UK) was given at a dosage of 0.1 mg/kg subcutaneously. A single dose of enrofloxacin 10 mg/kg (Baytril, Bayer Hispania, Barcelona, Spain) was also administered as antibiotic prophylaxis. The experimental animals were connected to a breathing machine (New Generation Black Mk-TCIII, NSS, UK) for anesthetic maintenance with an oxygen flow of 0.7–0.8 L/min and vaporized isoflurane 2–2.5% at 3.5 L/min. Additionally, 1 ml of 4% articaine with 1:100,000 adrenaline (Ultracain, Laboratorios Normon, Tres Cantos, Madrid, Spain) was infiltrated in the mandibular zone.

After verifying the depth of anesthesia, the surgical area was disinfected with 10% topical povidone iodine (Iodine, Laboratorios Reig Jofré, Sant Joan Despí, Barcelona, Spain) and surgically dressed. The tail of the rat was immersed in hot water for 10 minutes and, after applying 70% ethanol, 1.5 ml of blood was collected from an incision.<sup>22</sup> Afterward, the animals were immobilized using a magnetic fixator retraction system (Fine Science Tools, Foster City, CA, USA).<sup>23</sup> A 1.5-cm long anteroposterior incision was made in the submandibular skin. After exposing the inferior border of the mandible through blunt dissection, a standardized rectangular bone defect (6 × 2 mm) was created following a previously described model.<sup>24</sup> Bone was removed with a rounded bur at 2000 rpm under sterile saline irrigation. Immediately after the mandibular bone defects were made, the envelopes with the alloca-

tion sequence were opened. In the experimental group, the bone defects were filled with metal particles up to the top of the defect. Metal particles gathered by implantoplasty of the coronal half of a 4.8 × 13 mm dental implant (Coral E.C., Avinent Implant System S.L., Santpedor, Spain) were inserted into the defect. The defects of positive controls were left empty. The wound was sutured with Vicryl 4-0 (Laboratorios Aragón, Barcelona, Spain). Figure 1 shows the surgical steps.

During the first 2 postoperative days, meloxicam 2 mg/kg (Metacam, Boehringer Ingelheim, Sant Cugat del Vallés, Barcelona, Spain) was administered subcutaneously every 24 h.

Thirty days after surgery, the animals underwent euthanasia by inhalation of a CO<sub>2</sub>-saturated atmosphere. Prior to euthanasia, the rats were anesthetized with 5% isoflurane as previously described. The same blood collection procedure was repeated to collect 1.5 ml of blood from the tail.

## 2.6 | Sample collection and processing

The sample of perilesional tissue obtained by dissection from the surgical site was immediately fixed with formaldehyde in 10% aqueous solution (order number HT501128-4L, Sigma-Aldrich, St. Louis, MO, USA). The blood, liver, spleen, brain and both lungs were extracted and frozen at -80°C for subsequent lyophilization.

Lyophilization is a process that aims to separate water (or some other solvent) from a solution by freezing and sublimation of the ice at reduced pressure. This procedure is the best method for drying organic compounds without altering their qualitative or quantitative composition.



## 2.7 | Quantification of metal ions

The quantitative analysis of Ti, Al, and V ions in blood and organs was performed by investigators unaware of the allocation of each sample.

### 2.7.1 | Instrumentation

Microwave-assisted digestions were performed in an Ethos 1 system (Milestone, Sorisole, Italy) equipped with TFM microsampling inserts for lower sample consumption and dilution. The ICP-MS measurements were carried out in an iCAP TQ triple-quadrupole instrument (Thermo Fisher Scientific, Waltham, MA, USA). The TQ-ICP-MS was fitted with a micromist nebulizer, a cyclonic spray chamber and copper/nickel sampling and skimmer cones. The samples, digestion reagents and final dilutions were weighed in an analytical balance (Mettler Toledo, Chicago, IL, USA) with  $\pm 0.1$  mg accuracy.

### 2.7.2 | Reagents

Ultrapure water ( $<18$  M $\Omega$ ·cm) obtained from a PURELAB flex 3 system (ELGA VEOLIA, Lane End, High Wycombe, UK) was used for all solutions and working standards. Concentrated nitric acid (HNO<sub>3</sub>) of analytical grade was purchased from Thermo Fisher Scientific (Waltham, MA, USA) and purified by sub-boiling distillation. Hydrogen peroxide (H<sub>2</sub>O<sub>2</sub>) as a 30% solution was obtained from Thermo Fisher Scientific (Waltham, MA, USA). Hydrofluoric acid (HF) 99.99% (metal basis purity) from Alfa Aesar was purchased from Fisher Scientific (Hampton, USA).

Contamination from reagents and vessels used for the digestion of the tissues was minimized by careful manipulation. At the beginning, hydrogen peroxide was not used, since it did not provide any significant improvement in the recoveries and in the repetition RSD (relative standard deviation) was higher. The purification of concentrated nitric acid by sub-boiling distillation was carried in the LO setting (lowest distillation rate) and an initial cleaning protocol to produce trace metal grade acid was performed using a double distillation of ultrapure water. In addition, when collecting the Milli-Q water used for further dilution of standards and samples, the first 500 ml were discarded. Clean-up of the polypropylene containers (used for dilution of the samples prior to their analysis by ICP-MS) with 1% nitric acid was conducted overnight. Subsequently, they were rinsed with Milli-Q water before sample preparation.

TABLE 1 Microwave digestion programs

	For organs	For blood
<b>Step 1</b>	10 min room temperature to 90°C	15 min room temperature to 90°C
<b>Step 2</b>	6 min 90 to 140°C	15 min 90 to 140°C
<b>Step 3</b>	5 min 140 to 200°C	15 min 140 to 200°C
<b>Step 4</b>	10 min hold at 200°C	10 min hold at 200°C
<b>Step 5</b>	1 h cooling to room temperature	1 h cooling to room temperature

### 2.7.3 | Microwave-assisted digestion

The lyophilized samples were grinded using an agate mortar, and 0.1 g of each sample was placed in the microwave digestion inserts. Twenty-five microliter of HF were first added and allowed to react with the sample powder for 5 min. Then, 2 ml of HNO<sub>3</sub> were added and the samples were subjected to the microwave heating program specified in Table 1. The digested samples were finally diluted 10-times in 2% HNO<sub>3</sub>.<sup>20,25</sup>

Due to the more complex nature of the matrix in blood samples, 0.1 g of freeze-dried blood was incubated with 25  $\mu$ l of HF and 2 ml of HNO<sub>3</sub> for one hour at room temperature before applying the modified digestion program in the microwave, as shown in Table 1. The use of totally new sample vessels specially designed for microsamples intended to minimize external contamination. Between samples, the inserts were cleaned using 2 ml of 50% (v/v) HNO<sub>3</sub> and 25  $\mu$ l of concentrated HF. The MW heating program for the cleaning was carried out using 10 min ramp up to 150°C, 10 min hold at 150°C (MW power of 900 W in both steps) and a cooling step for 60 min up to room temperature. Afterward, inserts were rinsed with ultrapure water and dried before the next run.

### 2.7.4 | ICP-MS measurements

Ti was measured in the TQ-ICP-MS by monitoring the isotope <sup>47</sup>Ti<sup>+</sup> to avoid interference of the long half-life <sup>48</sup>Ca<sup>+</sup> isotope on the most abundant isotope <sup>48</sup>Ti<sup>+</sup>. The analysis was carried out in triple-quadrupole (TQ) mode using oxygen in the second quadrupole to form <sup>47</sup>Ti<sup>16</sup>O<sup>+</sup>, which is monitored in the m/z 63. Vanadium was also measured as its most abundant oxide, <sup>51</sup>V<sup>16</sup>O<sup>+</sup>, in TQ-O<sub>2</sub> mode, at m/z 67. Aluminum was measured in single-quadrupole (SQ) mode as <sup>27</sup>Al<sup>+</sup>. All analyses were quantified by external calibration using elemental standards, and scandium was used as internal standard. The sample measurement time was 2 min per sample and the calibration curve was prepared for Ti, Al and V with standards of 0, 0.25, 0.50, 1, 2.5, and 5 ng g<sup>-1</sup> (solutions prepared by weight). The

instrumental detection limit estimated as  $3\sigma$  (blanks)/slope of the calibration curve was  $0.007 \text{ ng Ti ml}^{-1}$ ,  $0.158 \text{ ng Al ml}^{-1}$  and  $0.002 \text{ ng V ml}^{-1}$ . Sensitivity (slope of the calibration curve) for Ti is  $69000 \text{ cps/ppb}$  ( $r^2 = 0.9992$ ), which is extremely low. However, considering the dilutions conducted in the samples this translated into 1.75, 39, and  $0.51 \text{ ng g}^{-1}$  of tissue for Ti, Al, and V, respectively. The measurement of each prepared sample was done by triplicate, and for every organ a duplicate of the digestion was prepared. Reproducibility within measured replicates was between 2% and 3% in all cases and between procedure replicates (including digestion) below 15% for the three elements.

## 2.8 | Histological samples

Histological analysis of the perilesional tissue of the surgical site was performed by an experienced pathologist (S.B.). The tissue was fixed in 10% neutral buffered formalin and embedded in paraffin after decalcification.<sup>26</sup> Then, paraffin blocks were sectioned using a Microm HM 340 E rotatory microtome (Thermo Fisher Scientific, Wall-dorf, Germany) to a thickness of  $5 \mu\text{m}$  for staining with hematoxylin-eosin (HE).

A light microscope (CX31, Olympus, Tokyo, Japan) was used to study the histological samples. In addition, a Leica DMD 108 microscope (Leica Company, Wetzlar, Germany) was used to obtain microphotographs.

## 2.9 | Statistical analysis

The data obtained were entered in a Microsoft Excel spreadsheet (Microsoft, Redmond, WA, USA) and processed using the Stata 14 statistical package (StataCorp, College Station, TX, USA).

For the descriptive analysis, the median and interquartile range (IQR) were calculated. Differences between groups were tested with the Mann-Whitney U-test, and within-subject changes were assessed with the Wilcoxon test. Regarding the analysis of metal ions, extreme outliers (defined as values above the 75th percentile and three times the IQR) were detected. We conducted the statistical analysis with and without these outliers. Finally, data were presented without outliers. In all cases, statistical significance was considered for  $p \leq 0.05$ .

## 3 | RESULTS

Of the 20 rats that underwent surgery, one in the positive control group died during the first 24 h of the postoperative period. Thus, ion quantification and histological analysis of the samples were finally carried out in 10 rats of the

experimental group, seven of the positive control group, and two of the negative control group.

### 3.1 | Quantification of metal ions

The distribution of metal ion concentrations in blood and organs is shown in Figure 2. Tables 2 and 3 display the concentration of metal ions in blood and organs, respectively. These data were presented without the outlier values.

#### 3.1.1 | Blood

There were no statistically significant differences between the study groups in terms of Ti, Al, or V ion concentrations. However, in the experimental group the concentration of Al was significantly lower in the post-intervention sample compared to the pre-intervention sample (Table 2).

The two rats of the negative control group (not operated) showed the following concentrations of metal ions in the pre-intervention sample: range [Ti] =  $160.5\text{--}371.3 \text{ ng/g}$ ; range [Al] =  $747.9\text{--}758.3 \text{ ng/g}$ ; range [V] =  $4.12\text{--}14.6 \text{ ng/g}$ , while the post-intervention concentrations were: range [Ti] =  $149.6\text{--}165.4 \text{ ng/g}$ ; range [Al] =  $689.0\text{--}1149.5 \text{ ng/g}$ ; range [V] =  $4.9\text{--}5.3 \text{ ng/g}$ .

#### 3.1.2 | Visceral tissues

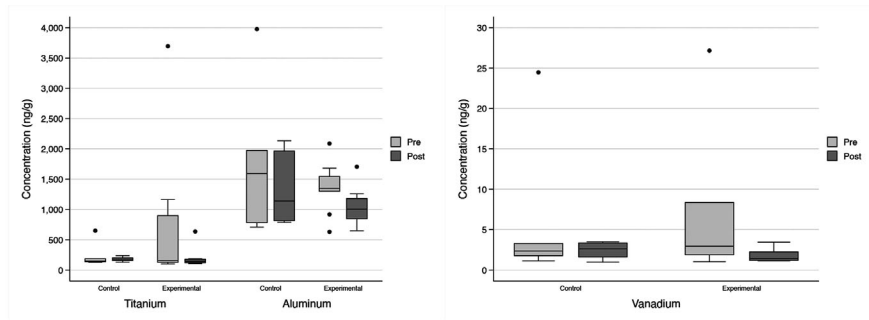
The concentrations of Ti ions in brain ( $p = 0.010$ ), spleen ( $p = 0.037$ ) and liver ( $p = 0.014$ ) were significantly higher in the experimental group than in the positive controls (Table 3). In addition, there also was a higher concentration of V ions in the brain of the experimental rats ( $p = 0.016$ ; Table 3). There were no statistically significant differences in Al ion concentrations (Table 3).

The concentrations of metal ions are reported in parentheses for the two rats of the negative control group in brain (range [Ti] =  $420.4\text{--}497.0 \text{ ng/g}$ ; range [Al] =  $1254.5\text{--}1858.6 \text{ ng/g}$ ; range [V] =  $5.7\text{--}7.2 \text{ ng/g}$ ), spleen (range [Ti] =  $421.9\text{--}447.1 \text{ ng/g}$ ; range [Al] =  $1113.6\text{--}1133.7 \text{ ng/g}$ ; range [V] =  $37.3\text{--}55.0 \text{ ng/g}$ ), lungs (range [Ti] =  $291.4\text{--}318.7 \text{ ng/g}$ ; range [Al] =  $1555.2\text{--}2203.6 \text{ ng/g}$ ; range [V] =  $8.4\text{--}11.0 \text{ ng/g}$ ) and liver (range [Ti] =  $374.1\text{--}493.7 \text{ ng/g}$ ; range [Al] =  $751.0\text{--}1160.6 \text{ ng/g}$ ; range [V] =  $9.4\text{--}10.4 \text{ ng/g}$ ).

### 3.2 | Histological samples

All specimens consisted of mucosa lined by squamous epithelium, submucosa, skeletal muscle, accessory salivary glands, alveolar bone, and teeth.

(A) Blood



(B) Organs

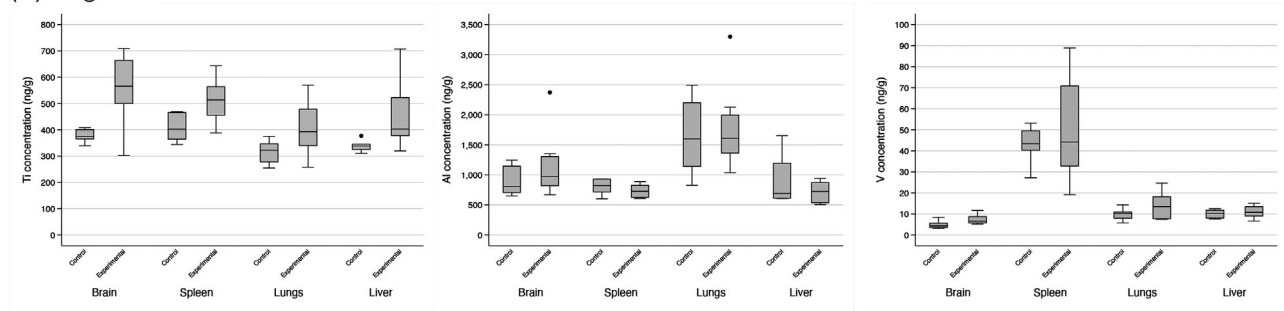


FIGURE 2 Boxplots of titanium, aluminum, and vanadium ion concentrations in blood (A) and organs (B)

TABLE 2 Results of the quantification of ions in blood: Data expressed as median (IQR)

Study groups			Between-group comparison	Within-group comparison	
	Quantification of ions	Experimental	Positive control	p-value experimental versus control group	p-value experimental group pre-intervention versus post-intervention
<b>Blood, ng/g</b>					
<b>Pre-intervention</b>					
Titanium (n = 17)	157.9 (769.3)	148.05 (50.3)		0.939	
Aluminum (n = 18)	1347.9 (245.9)	1593.7 (1192.1)		0.9854	
Vanadium (n = 16)	2.95 (6.47)	2.36 (1.5)		0.755	
<b>Post-intervention</b>					
Titanium (n = 17)	145.4 (59.3)	165.6 (44.4)		0.746	0.161
Aluminum (n = 18)	1004.5 (334.9)	1138.3 (1149.8)		0.731	0.028*
Vanadium (n = 16)	1.43 (1.05)	2.64 (1.75)		0.682	0.917

\*statistically significant ( $p < 0.05$ ).

In the experimental group, metal particles were present as black deposits of irregular contour and birefringent under polarized light. As shown in Figure 3A, there was a granulomatous reaction with the presence of histiocytes and multinucleated giant cells (MNGCs) around the metal particles. Small metal particles were found within the cytoplasm of the MNGCs (Figure 3B).

Disordered mature bone with irregular ossification lines corresponding to a fracture bone callus was detected in all

specimens of the experimental and positive control groups (Figure 3C).

#### 4 | DISCUSSION

The present study evaluated whether the implantation of metal particles in a mandibular defect in rats resulted in the dissemination of metal ions to the blood, liver, spleen,

TABLE 3 Results of the quantification of ions in organs: Data expressed as median (IQR)

Quantification of ions	Study groups		Between-group comparison <i>p</i> -value experimental versus control group
	Experimental	Positive control	
<b>Organs, ng/g</b>			
<b>Brain</b>			
Titanium ( <i>n</i> = 19)	565.6 (163.2)	374.6 (35.6)	0.010*
Aluminum ( <i>n</i> = 19)	971.1 (487.3)	806.6 (440.5)	0.512
Vanadium ( <i>n</i> = 19)	6.5 (3.1)	4.3 (2.0)	0.016*
<b>Spleen</b>			
Titanium ( <i>n</i> = 19)	513.3 (108.2)	402.5 (100.9)	0.037*
Aluminum ( <i>n</i> = 17)	726.0 (201.5)	819.9 (214.6)	0.721
Vanadium ( <i>n</i> = 18)	44.2 (38.1)	43.4 (9.2)	0.988
<b>Lungs</b>			
Titanium ( <i>n</i> = 18)	392.7 (138.8)	322.3 (69.0)	0.135
Aluminum ( <i>n</i> = 18)	1610.2 (633.9)	1599.7 (1060.8)	0.988
Vanadium ( <i>n</i> = 18)	13.4 (10.4)	10.2 (3.0)	0.632
<b>Liver</b>			
Titanium ( <i>n</i> = 18)	402.8 (145)	338.7 (20.4)	0.014*
Aluminum ( <i>n</i> = 19)	723.5 (337.2)	689.3 (584.5)	0.978
Vanadium ( <i>n</i> = 19)	10.8 (4.4)	10.3 (3.8)	0.940

\*statistically significant ( $p < 0.05$ ).

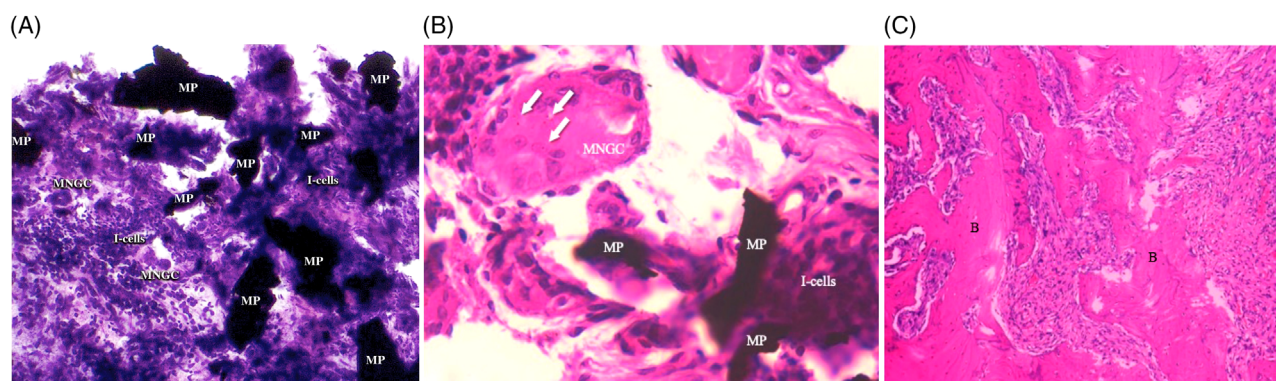


FIGURE 3 Granulomatous reaction with the presence of histiocytes and multinucleated giant cells around metal particles. MNGCs, multinucleated giant cells; MP, metal particle; I-cells, inflammatory cells. Hematoxylin-eosin staining; magnification  $\times 20$ . (A) Small metal particles within the cytoplasm of the multinucleated giant cells (arrows). MNGCs, multinucleated giant cells; MP, metal particle; I-cells, inflammatory cells. Hematoxylin-eosin staining; magnification  $\times 63$ . (B) Disordered mature bone with irregular ossification lines corresponding to a fracture bone callus. B, bone. Hematoxylin-eosin staining; magnification  $\times 10$  (C)

lungs, and brain 30 days after surgery. To our knowledge, this is the first study to quantify the accumulation of metal ions in distant organs after the implantation of Ti metal particles from dental implants. The results obtained indicate a higher concentration of Ti ions in the liver, spleen, and brain of the rats in the experimental group compared to the positive control group. There was also a higher concentration of V ions in the brain of the experimental rats. On the other hand, the histological findings suggest that

the metal debris induced a granulomatous reaction with the presence of histiocytes and MNGCs characteristic of a foreign body reaction.

The present study has some limitations that should be commented on. First, the study period was only 30 days; as a result, the effects of these particles over the middle and long term are not known. Second, the experimental rats had a mandibular defect that was filled with metal particles. Although this model does not mimic the clinical



situation in implantoplasty, the mobilization of metal ions from the implanted site to organs and the local reaction simulate a clinical scenario, in which debris cannot be fully removed from the surgical field. On the other hand, the presence of Ti, Al, and V ions could come from other sources, and the variations of these ions might not be explained only by the presence of implant debris. These ions, especially Ti and Al, are difficult to measure due to the high environmental backgrounds coming, most likely, from food and drinking water. Ti dioxide is a common food additive (also for humans), although recently banned by the European Union (EU).<sup>27</sup> In addition, the presence of Ti in waters has been well documented.<sup>27</sup> Therefore, small variations due to the Ti metal particles above the relatively high blanks are expected to hamper ultratrace analysis. Similar reasons can be given for Al determination.<sup>20,28</sup> It is worth noting that outliers were removed from the analysis because statistical power was over 80% even after removal, and analysis with and without outliers yielded the same significance of results. Negative control rats had a higher concentration of some metal ions than positive controls, which possibly reflects that rats did not have feeding difficulties.

Commercially pure Ti or Ti alloy is commonly used in dental implants and orthopedics due to its corrosion resistance, biocompatibility, and mechanical properties.<sup>29</sup> Although Ti has been typically regarded as inert, several studies have reported that Ti implants can undergo corrosion and wear, releasing metal particles into the medium.<sup>30</sup> Such metal debris can be transported to other tissues, and may even lead to adverse events including cytotoxicity, genotoxicity, carcinogenicity, and metal hypersensitivity.<sup>20,28</sup> In the present study, dissemination of Ti and V ions from the mandibular defect to certain organs of the rat was observed 30 days after the implantation of these metal particles. There was a decrease in the concentration of Al ions in the blood of the experimental group. Indeed, concentration of aluminum ions in the positive control group decreased across time, although the difference was not statistically significant. Therefore, both groups appear to have a decrease in serum aluminum levels, which might be due to the ubiquitous nature of aluminum.<sup>31</sup> It must be pointed out that the concentration of metal ions in the different tissues was low (ng/g), and that their potential clinical effects are still unknown. Future studies should address the effects of the accumulation of these metal ions since Ti nanoparticles and ions may exert cytotoxic effects upon human cells.<sup>28</sup>

Some authors have suggested that bone loss around dental implants may be caused or accelerated by an inflammatory reaction in response to the presence of metal particles or ions.<sup>5,6</sup> In fact, Ti particles and ions are more common in peri-implantitis sites and can cause dysbiosis

of the peri-implant biofilm.<sup>32</sup> There are several mechanisms by which metal particles can be released into the peri-implant environment, such as implant insertion,<sup>33</sup> micromovements of the implant in the bone,<sup>34</sup> the methods used to decontaminate peri-implant surfaces<sup>26</sup> or biocorrosion.<sup>35</sup> Among these mechanisms, implantoplasty is undoubtedly the technique that releases the greatest amount of metal particles into the peri-implant environment. Barrak et al.,<sup>36</sup> in an *in vitro* study, reported that irregularly shaped micro- and nanoparticles are released during implantoplasty. In addition, these authors found that Ti-6Al-4V particles caused a greater reduction of fibroblast cell viability compared to commercially pure Ti. In this line, a recent study showed that the same metal particles used in the present study exhibited cytotoxic effects in the fibroblast cell assays in the undiluted extract, but not in the diluted extracts.<sup>37</sup>

Our results show that the metal particles embedded in an experimental rat jaw defect triggered chronic inflammation with a foreign body granulomatous reaction characterized by the presence of histiocytes and MNGCs. On the other hand, a bone callus was observed in all the histological samples of the experimental and positive control groups, which did not differ between the study groups. Schwarz et al.<sup>38</sup> conducted an experimental study in six dogs and histologically examined the effect of Ti metal particles released during implantoplasty around the dental implants. They reported a moderate deposition of Ti particles surrounded by highly vascularized areas delimited by a mixed chronic inflammatory cell infiltrate. Other authors<sup>39–42</sup> reported that Ti metal particles induce a chronic inflammatory cell infiltrate associated to a foreign body reaction, which is in line with the results of our study. Future studies should consider the evaluation of the inflammatory process in the subepithelial connective tissue around metal particles, for instance by quantifying proinflammatory cytokines.

In the field of orthopedics, metal particles and ions induce immune responses leading to osteolysis around the prosthesis in an absence of bacteria—a condition known as aseptic osteolysis.<sup>43</sup> Friction between the joint surfaces causes wear of the prosthesis, and the released metal particles induce a local periprosthetic osteolytic reaction.<sup>44</sup> This complication predominantly occurs 5 years post-orthopedic implantation<sup>43</sup> and is characterized by histiocytic inflammation and activation of osteoclasts, leading to osteolysis and consequently joint prosthesis failure.<sup>45</sup> Histologically, a granulomatous reaction is observed, with black and birefringent particles.<sup>42</sup> These findings are consistent with the histological findings in our experimental rats. Thus, metal particles embedded in a mandible may have a detrimental effect upon the peri-implant tissues, and the mechanism involved could be similar to that



observed in total joint replacement surgery. Indeed, bone loss around dental implants may be increased due to the abundance of bacteria in the mouth.<sup>33</sup> However, long-term studies and methodologies that mimic the real scenario are still required to determine the effects of these metallic particles upon implant survival.

## 5 | CONCLUSION

In summary, 1 month after implantation of Ti metal particles, we observed a granulomatous inflammatory reaction with the presence of histiocytes and MNGCs. In addition, the concentration of Ti ions increased in the liver, spleen, and brain, as the concentration of vanadium ions in the brain.

## ACKNOWLEDGMENTS AND CONFLICTS OF INTEREST

This study was supported by the Instituto de Salud Carlos III through project PI20/01596 (co-funded by the European Regional Development Fund [ERDF], a way to build Europe).

The authors thank the CERCA Program / Generalitat de Catalunya for institutional support.

The authors thank Dr. Samira Bakali Badesa, the pathologist who studied the histological specimens, for her help and assistance.

The authors thank Prof. Dr. Albert Soler-Gil (MAiMA Group) for his help in lyophilization of the samples.

Jorge Toledano-Serrabona has received no grants, personal fees, or financial support.

Diogo Pompéu de Moraes kindly acknowledges the Coordenação de Aperfeiçoamento de Pessoal de Nível Superior – Brasil (CAPES) – Finance Code 001 for scholarship.

Mario Corte-Rodríguez reports grants from the government of Asturias through the “Consejería de Empleo, Industria y Turismo del Principado de Asturias” co-financed by FEDER funds (ref. SV-PA-21-AYUD/2021/51399), the funding from the Spanish Ministry of Economy, Industry and Competitiveness (MINECO) through project PID2019-104334RB-I00. Mario Corte-Rodríguez acknowledges the Instituto de Salud Carlos III for the postdoctoral Sara Borrell contract (CD19/00249).

María Montes-Bayón reports grants from the government of Asturias through the “Consejería de Empleo, Industria y Turismo del Principado de Asturias” co-financed by FEDER funds (ref. SV-PA-21-AYUD/2021/51399), the funding from the Spanish Ministry of Economy, Industry and Competitiveness (MINECO) through project PID2019-104334RB-I00.

Octavi Camps-Font reports grants from Instituto de Salud Carlos III during the conduct of the study. Octavi Camps-Font reports grants, personal fees, and non-financial support from Avinent (Santpedor, Spain) outside the submitted work. Camps-Font has participated as co-investigator in clinical trials sponsored by Mundipharma (Cambridge, UK) and Menarini Recherche (Florence, Italy).

Eduard Valmaseda-Castellón reports grants from Instituto de Salud Carlos III during the conduct of the study. Eduard Valmaseda-Castellón reports personal fees and non-financial support from MozoGrau (Valladolid, Spain). He has received personal fees from BioHorizons Ibérica (Madrid, Spain), Inibsa Dental (Lliça de Vall, Spain), and Dentsply Implants Iberia (Barcelona, Spain) outside the submitted work. Valmaseda-Castellón is the director of the Avinent-University of Barcelona research agreement (Càtedra UB-Avinent). In addition, Valmaseda-Castellón has participated as an investigator in clinical trials sponsored by Mundipharma (Cambridge, UK) and Geistlich (Wolhusen, Switzerland) outside the submitted work.

Cosme Gay-Escoda reports grants from Instituto de Salud Carlos III during the conduct of the study. Cosme Gay-Escoda reports grants, personal fees, and non-financial support from Mundipharma (Cambridge, UK) and Menarini Recherche (Florence, Italy) outside the submitted work.

M<sup>a</sup> Ángeles Sánchez-Garcés reports grants from Instituto de Salud Carlos III during the conduct of the study. M<sup>a</sup> Ángeles Sánchez-Garcés reports personal fees from Nobel Biocare (Göteborg, Sweden), Zimmer Biomet (Warsaw, IN, USA), and Menarini Recherche (Florence, Italy) outside the submitted work.


## AUTHOR CONTRIBUTIONS

Jorge Toledano-Serrabona: contributed to conception, design, data acquisition and interpretation, and drafted the manuscript. Octavi Camps-Font: contributed to design, data interpretation, and critically reviewed the manuscript. Diogo Pompéu de Moraes and María Montes-Bayón: contributed to data acquisition and interpretation, and critically reviewed the manuscript. Mario Corte-Rodríguez: contributed to data acquisition and critically reviewed the manuscript. Eduard Valmaseda-Castellón: contributed to design, data acquisition and interpretation, and critically reviewed the manuscript. Cosme Gay-Escoda: contributed to conception, design, and critically reviewed the manuscript. María Ángeles Sánchez-Garcés: contributed to conception, design, data acquisition, and critically reviewed the manuscript. All authors gave final approval and agree to be accountable for all aspects of the work.



## ORCID

Jorge Toledano-Serrabona  <https://orcid.org/0000-0002-0166-8876>

Octavi Camps-Font  <https://orcid.org/0000-0001-9991-2226>

Diogo Pompéu de Moraes  <https://orcid.org/0000-0003-4992-5226>

Mario Corte-Rodríguez  <https://orcid.org/0000-0003-0109-4101>

María Montes-Bayón  <https://orcid.org/0000-0001-6114-9405>

Eduard Valmaseda-Castellón  <https://orcid.org/0000-0001-9669-3187>

Cosme Gay-Escoda  <https://orcid.org/0000-0002-6812-024X>

M. Ángeles Sánchez-Garcés  <https://orcid.org/0000-0002-8818-7142>

## REFERENCES

- Barrak F, Li S, Muntane A, Bhatia M, Crossthwaite K, Jones J. Particle release from dental implants immediately after placement—an ex vivo comparison of different implant systems. *Dent Mater*. 2022;38(6):1004-1014.
- Moraschini V, Poubel LA da C, Ferreira VF, Barboza E dos SP. Evaluation of survival and success rates of dental implants reported in longitudinal studies with a follow-up period of at least 10 years: a systematic review. *Int J Oral Maxillofac Surg*. 2015;44(3):377-88.
- Rakic M, Galindo-Moreno P, Monje A, et al. How frequent does peri-implantitis occur? A systematic review and meta-analysis. *Clin Oral Investig*. 2018;22:1805-16.
- Schwarz F, Schwarz F, Derks J, Monje A, Wang HL. Peri-implantitis. *J Periodontol*. 2018;89:S267-290.
- Fretwurst T, Nelson K, Tarnow DP, Wang HL, Giannobile WV. Is metal particle release associated with peri-implant bone destruction? An emerging concept. *J Dent Res*. 2018;97:259-265.
- Wilson TG. Bone loss around implants—is it metallosis? *J Periodontol*. 2021;92:181-185.
- Hanawa T. Titanium-tissue interface reaction and its control with surface treatment. *Front Bioeng Biotechnol*. 2019;7:170.
- Apaza-Bedoya K, Tarce M, Benfatti CAM, et al. Synergistic interactions between corrosion and wear at titanium-based dental implant connections: a scoping review. *J Periodontol Res*. 2017;52:946-54.
- Toledano-Serrabona J, Sánchez-Garcés MÁ, Gay-Escoda C, et al. Mechanical properties and corrosion behavior of Ti6Al4V particles obtained by implantoplasty: an in vitro study. Part II. *Materials (Basel)*. 2021;14:6519.
- Mathew MT, Kerwell S, Lundberg HJ, Sukotjo C, Mercuri LG. Tribocorrosion and oral and maxillofacial surgical devices. *Br J Oral Maxillofac Surg*. 2014;52:396-400.
- Noronha Oliveira M, Schunemann WVH, Mathew MT, et al. Can degradation products released from dental implants affect peri-implant tissues? *J Periodontol Res*. 2018;53:1-11.
- Tinoco AD, Saxena M, Sharma S, et al. Unusual synergism of transferrin and citrate in the regulation of Ti(IV) speciation, transport, and toxicity. *J Am Chem Soc*. 2016;138:5659-5665.
- Suárez-López del Amo F, Rudek I, Wagner V, et al. Titanium activates the DNA damage response pathway in oral epithelial cells: a pilot study. *Int J Oral Maxillofac Implants*. 2017;32:1413-1420.
- Kotsakis GA, Black R, Kum J, et al. Effect of implant cleaning on titanium particle dissolution and cytocompatibility. *J Periodontol*. 2021;92:580-591.
- Rakic M, Radunovic M, Petkovic-Curcin A, Tatic Z, Basta-Jovanovic G, Sanz M. Study on the immunopathological effect of titanium particles in peri-implantitis granulation tissue: a case-control study. *Clinical Oral Implants Res*. 2022;33(6):656-666.
- Albrektsson T, Dahlin C, Jemt T, Sennerby L, Turri A, Wennerberg A. Is marginal bone loss around oral implants the result of a provoked foreign body reaction? *Clin Implant Dent Relat Res*. 2014;16:155-165.
- Swiatkowska I, Martin N, Hart AJ. Blood titanium level as a biomarker of orthopaedic implant wear. *J Trace Elem Med Biol*. 2019;53:120-128.
- Heyman O, Koren N, Mizraji G, et al. Impaired differentiation of Langerhans cells in the murine oral epithelium adjacent to titanium dental implants. *Front Immunol*. 2018;9:1-14.
- Kilkenny C, Browne WJ, Cuthill IC, Emerson M, Altman DG. Improving bioscience research reporting: the ARRIVE guidelines for reporting animal research. *PLoS Biol*. 2010;8:e1000412.
- Sarmiento-González A, Encinar JR, Marchante-Gayón JM, Sanz-Medel A. Titanium levels in the organs and blood of rats with a titanium implant, in the absence of wear, as determined by double-focusing ICP-MS. *Anal Bioanal Chem*. 2009;393:335-343.
- Costa-Berenguer X, García-García M, Sánchez-Torres A, Sanz-Alonso M, Figueiredo R, Valmaseda-Castellón E. Effect of implantoplasty on fracture resistance and surface roughness of standard diameter dental implants. *Clin Oral Implants Res*. 2018;29:46-54.
- Removal of blood from laboratory mammals and birds. First report of the BVA/FAME/RSPCA/UFPAW Joint Working Group on Refinement. *Lab Anim*. 1993;27:1-22.
- Padiá-Molina M, Rodríguez JC, Volk SL, Rios HF. Standardized in vivo model for studying novel regenerative approaches for multitissue bone-ligament interfaces. *Nat Protoc*. 2015;10:1038-1049.
- Liu G, Guo Y, Zhang L, et al. A standardized rat burr hole defect model to study maxillofacial bone regeneration. *Acta Biomater*. 2019;86:450-464.
- Taboada-López MV, Iglesias-López S, Herbelo-Hermelo P, Bermejo-Barrera P, Moreda-Piñeiro A. Ultrasound assisted enzymatic hydrolysis for isolating titanium dioxide nanoparticles from bivalve mollusk before sp-ICP-MS. *Anal Chim Acta*. 2018;1018:16-25.
- Liu H, Zhu R, Liu C, et al. Evaluation of decalcification techniques for rat femurs using he and immunohistochemical staining. *Biomed Res Int*. 2017;2017:9050754.
- Candás-Zapico S, Kutscher DJ, Montes-Bayón M, Bettmer J. Single particle analysis of TiO<sub>2</sub> in candy products using triple quadrupole ICP-MS. *Talanta*. 2018;180:309-315.
- Soto-Alvaredo J, Blanco E, Bettmer J, et al. Evaluation of the biological effect of Ti generated debris from metal implants: ions and nanoparticles. *Metallomics*. 2014;6:1702-1708.



29. Siddiqi A, Payne AGT, De Silva RK, Duncan WJ. Titanium allergy: could it affect dental implant integration? *Clin Oral Implants Res.* 2011;22:673-680.
30. Wachi T, Shuto T, Shinohara Y, Matono Y, Makihira S. Release of titanium ions from an implant surface and their effect on cytokine production related to alveolar bone resorption. *Toxicology.* 2015;327:1-9.
31. Peydayesh M, Pauchard M, Bolisetty S, Stellacci F, Mezzenga R. Ubiquitous aluminium contamination in water and amyloid hybrid membranes as a sustainable possible solution. *Chem Commun.* 2019;55:11143-11146.
32. Souza JGS, Costa Oliveira BE, Bertolini M, et al. Titanium particles and ions favor dysbiosis in oral biofilms. *J Periodontol Res.* 2020;55:258-266.
33. Silva GAF, Faot F, da Silva WJ, Del Bel Cury AA. Does implant surface hydrophilicity influence the maintenance of surface integrity after insertion into low-density artificial bone? *Dent Mater.* 2021;37:69-84.
34. Sridhar S, Wang F, Wilson TG, Palmer K, Valderrama P, Rodrigues DC. The role of bacterial biofilm and mechanical forces in modulating dental implant failures. *J Mech Behav Biomed Mater.* 2019;92:118-127.
35. Mombelli A, Hashim D, Cionca N. What is the impact of titanium particles and biocorrosion on implant survival and complications? A critical review. *Clin Oral Implants Res.* 2018;29:37-53.
36. Barrak FN, Li S, Muntane AM, Jones JR. Particle release from implantoplasty of dental implants and impact on cells. *Int J Implant Dent.* 2020;6:1-9.
37. Toledano-Serrabona J, Gil FJ, Camps-Font O, Valmaseda-Castellón E, Gay-Escoda C, Sánchez-Garcés MÁ. Physicochemical and biological characterization of Ti6Al4V particles obtained by implantoplasty: an in vitro Study. Part I. *Materials (Basel)* 2021;14:6507.
38. Schwarz F, Sahm N, Mihatovic I, Golubovic V, Becker J. Surgical therapy of advanced ligature-induced peri-implantitis defects: cone-beam computed tomographic and histological analysis. *J Clin Periodontol.* 2011;38:939-949.
39. Eger M, Sterer N, Liron T, Kohavi D, Gabet Y. Scaling of titanium implants entrains inflammation-induced osteolysis. *Sci Rep.* 2017;7:1-11.
40. Wang X, Li Y, Feng Y, Cheng H, Li D. Macrophage polarization in aseptic bone resorption around dental implants induced by Ti particles in a murine model. *J Periodontol Res.* 2019;54:329-338.
41. Pisanu F, Andreozzi M, Fiori E, et al. Surgical management of hip prosthetic failure in metallosis: a case series and literature review. *J Orthop.* 2021;28:10-20.
42. Cipriano CA, Issack PS, Beksac B, Della Valle AG, Sculco TP, Salvati EA. Metallosis after metal-on-polyethylene total hip arthroplasty. *Am J Orthop (Belle Mead NJ).* 2008;37:18-25.
43. Lohmann CH, Singh G, Willert H-G, Buchhorn GH. Metallic debris from metal-on-metal total hip arthroplasty regulates periprosthetic tissues. *World J Orthop.* 2014;5:660-666.
44. Bitar D, Parvizi J. Biological response to prosthetic debris. *World J Orthop.* 2015;6:172-189.
45. Holt G, Murnaghan C, Reilly J, Meek RM. The biology of aseptic osteolysis. *Clin Orthop Relat Res.* 2007;460:240-252.

**How to cite this article:** Toledano-Serrabona J, Camps-Font O, de Moraes DP, et al. Ion release and local effects of titanium metal particles from dental implants: An experimental study in rats. *J Periodontol.* 2023;94:119–129.  
<https://doi.org/10.1002/JPER.22-0091>